JOURNAL OF MASS SPECTROMETRY, VOL. 33, 25–34 (1998)

Energetics of the Cyclo(Pro–Gly) Cation Fragmentation: a Mass spectrometric Study and Theoretical Calculations

Yun Ling and Chava Lifshitz*
Department of Physical Chemistry and The Farkas Center for Light-Induced Processes, The Hebrew University of Jerusalem, Jerusalem 91904, Israel

The energetics of HNCO elimination from the cyclo(Pro–Gly) radical cation was studied by electron ionization tandem mass spectrometry, photoionization mass spectrometry and RRKM/QET modeling. The heat of formation and vibrational frequencies of the reactant were calculated by density functional theory (DFT). Homodesmotic reactions involving cyclo(Pro–Gly) were used to derive its heat of formation at 0 K as -72.0 ± 3.0 kcal mol^{-1} (1 kcal = 4.184 kJ). Vibrational frequencies were calculated at the B3LYP/6–31G(d) level. The critical energy for HNCO loss was determined from the experiment, by modeling, to be 1.2 ± 0.1 eV. The heat of formation of the cyclo(Pro–Gly) radical cation and of the product ion $C_6H_9NO^{+\cdot}$ at 0 K were determined to be 130.9 ± 3.0 and $\leqslant 182.8 \pm 5.0$ kcal mol^{-1}, respectively. The salient features of the potential energy profile along the reaction coordinate were probed by DFT calculations. © 1998 John Wiley & Sons, Ltd.

J. Mass Spectrom. **33**, 25–34 (1998)

KEYWORDS: cyclic peptide; photoionization; kinetic energy release; RRKM/QET; density functional theory; ionization energy; appearance energy; critical energy; heats of formation

INTRODUCTION

Peptides are an important class of molecules in rational drug design for multiple reasons and cyclic dipeptide drugs have successfully entered clinical trials.[1] The mechanism of the fragmentation of small peptides is an important experimental objective for future pharmacological and toxicity studies.[1] The energetics and dynamics of ionic dissociations of small peptides have been topics of interest in recent years.[2–5] Most of the studies have been carried out on protonated[1–3] or deprotonated peptides.[4] Dissociation is mainly governed by the site of protonation or deprotonation. RRKM calculations were applied to understand the energetics of fragmentation.[2,4,6] Our present research deals with the radical cation of a cyclic dipeptide, cyclo(Pro–Gly) (**I**)

Fragmentations of protonated cyclic peptides have been studied by tandem mass spectrometry (MS/MS).[7] Cyclic dipeptides (diketopiperazines) can be eliminated from the *N*-termini of protonated tripeptides by collisionally activated dissociation (CAD).[8] This mechanism was identified by neutral fragment reionization mass spectra. The strongest peak in the collision-induced dissociative ionization (CIDI) spectra of diketopiperazine results from the loss of HN=C=O (*m/z* 43) from the molecular ion.

In this paper, we report on our first study of the energetics of small cyclic peptide cation fragmentation. The major primary decomposition reactions of cyclo(Pro–Gly) radical cation at low energy were found to be HNCO loss and CO elimination; the latter reaction was too weak for a photoionization measurement to be made.

The energetics of HNCO elimination from the cyclo(Pro–Gly) radical cation (see structure) were investigated by electron ionization MS/MS, photoionization mass spectrometry (PIMS) and RRKM/QET and DFT calculations and the results are reported here. RRKM modeling requires a knowledge of the heat of formation of the reactant neutral and the vibrational frequencies of the neutral and ion. These data were not available experimentally. We applied density functional theory (DFT)[9] to derive the heat of formation of the neutral and the vibrational frequencies of the neutral and radical cation. The heat of formation of the reactant radical cation was deduced from that of the neutral and from the measured ionization energy (*IE*) to be reported. We shall demonstrate that the HNCO elimination has a small kinetic shift.[10,11] Equating the critical energy of activation with the endothermicity of the reaction leads to an upper limit for the heat of the formation of the product ion, which will be shown to be in line with DFT calculations.

EXPERIMENTAL

Mass spectra and mass-analyzed ion kinetic energy (MIKE) spectra were measured on a VG ZAB-2F

* *Correspondence to*: C. Lifshitz, Department of Physical Chemistry and the Farkas Center for Light-Induced Processes, The Hebrew University of Jerusalem, Jerusalem 91904, Israel.

Contract grant sponsor: German–Israeli Foundation for Scientific Research and Development (GIF).

CCC 1076–5174/98/010025–10 $17.50

Received 10 June 1997
Accepted 15 September 1997

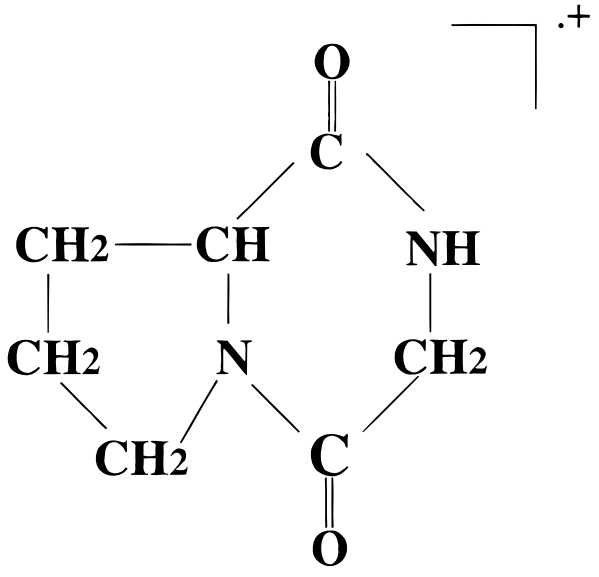

(I)

Cyclo(Pro-Gly)$^{\cdot+}$

double-focusing mass spectrometer of reverse geometry.[12] For MIKES, the magnetic field was set to select the ions of desired m/z value under investigation; ionic products of their decomposition in the second field-free region, between the magnetic and electrostatic analyzers, were detected by scanning the electric sector potential under conditions of good energy resolution with the energy-resolving β-slit partially closed. Kinetic energy release distributions (KERDs) were determined from first derivatives of metastable peak shapes and average KERs were deduced therefrom.[13]

The experimental technique of time-resolved photoionization mass spectrometry (TPIMS) has been described in detail recently.[14] Briefly, photoionization is induced by a pulsed vacuum UV light source, a Hinteregger discharge in hydrogen producing the many-line spectrum. Photoions are ejected from the ion source into a quadrupole mass filter by a drawout pulse. The ion lifetime sampled prior to dissociation in the present experiment is $\sim$24 μs. The outcome of the TPIMS experiment is photoionization efficiency (PIE) curves, from which *IE*s and appearance energies (*AE*s) can be deduced. These PIE curves can be modeled by RRKM/QET calculations to be described below.

Cyclo(Pro–Gly) was a commercial sample from sigma and was employed without further purification.

A simple Knudsen-type molecular effusive beam source for low-volatility compounds constructed earlier[15] was used to vaporize cyclo(Pro–Gly).

COMPUTATION

Calculations carried out involved determining structures, heats of formation and vibrational frequencies using DFT on the one hand and microcanonical rate energy dependences, breakdown curves and PIE curves, using RRKM/QET, on the other.

Isodesmic[16–18] and homodesmotic[19,20] reactions have been widely used to evaluate stabilization energies and heats of formation of various molecules. An isodesmic reaction is one in which there is a retention of the number of bonds of a given formal type (single, double, triple), but a change in the structural relationships between them. A homodesmotic reaction is one in which (i) there are equal numbers of C atoms in their various states of hybridization in reactants and products and (ii) there are equal numbers of C atoms with no, one, two and three H atoms attached in reactants and products.[19a] It has been demonstrated that homodesmotic reactions are better suited than isodesmic reactions to describe the strain energy (destabilization energy) of cyclic compounds.[19]

DFT B3LYP/6–31G(d) energies were obtained with the combination of Becke's three-parameter exchange functional[21] with the gradient-corrected correlation functional of Lee *et al.*[22] The very good performance of B3LYP for harmonic frequencies has been well known for some time.[23,24] A recent study[25] on harmonic vibrational frequencies compared the different theories and showed that one of the most successful procedures involves B3LYP/6–31G(d) and the scaling factors for obtaining the fundamental vibrational frequencies and zero-point vibrational energies (ZPVE) have been derived. The B3LYP/6–31G(d) method was employed in this work to calculate the vibrational frequencies of neutral and cationic species of cyclo(Pro–Gly) which are needed in the RRKM modeling of experimental PIE curves and thermochemical data calculations.

The geometry of each molecule was completely optimized at the B3LYP/6–31G(d) level of theory. Vibrational frequencies were computed for all optimized geometries.

All density functional and *ab initio* calculations were carried out using the Gaussian 94 package[26] running on a DEC Alpha Turbolaser 8400 at the Institute of Chemistry.

PIE curves were modeled by RRKM/QET calculations.[27] The microcanonical rate coefficients $k(E)$ were calculated as a function of energy by an RRKM program.[28] Computed B3LYP/6–31G(d) vibrational frequencies of the cyclo(Pro–Gly) radical cation were employed for the reactant. Vibrational frequencies of the transition state were varied to obtain the best agreement with experiment. Once the $k(E)$ dependence had been computed, we proceeded to calculate breakdown curves of the ions at 0 K. The 0 K breakdown curves were convoluted with the instrumental slit function, with the calculated thermal energy distribution at the temperature of the experiment calculated from the vibrational frequencies of the neutral and with the energy deposition function. The resultant curve represents the calculated first derivative of the PIE curve of the ion, provided that the threshold law for photoionization is a step function.[10] These curves were integrated to compare them with the experimental PIE curves.

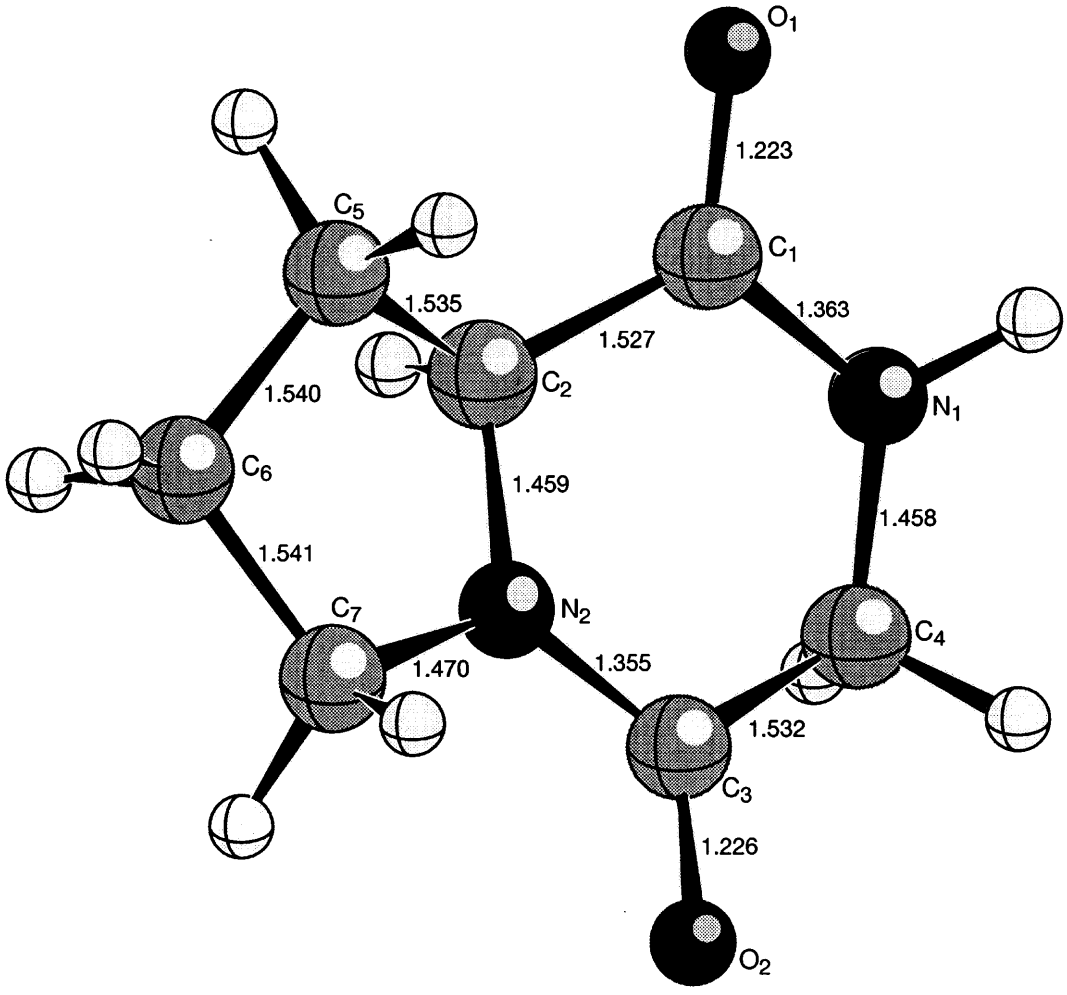

Figure 1. Geometry of cyclo(Pro–Gly) neutral, optimized at the B3LYP/6–31G(d) level.

RESULTS AND DISCUSSION

Geometry and vibrational frequencies of cyclo(Pro–Gly) neutral and cation

The vibrational frequencies of cyclo(Pro–Gly) neutral and cation were calculated at the B3LYP/6–31G(d) level. A scaling factor 0.9614 was adopted from Scott and Radom.[25] The optimized geometries of the cyclo(Pro–Gly) neutral and cation at the B3LYP/6–31G(d) level are shown in Figs 1 and 2, respectively. Both the neutral and cation have no symmetry (C_1). The bond lengths between heavy atoms are given. The bond length changes in the cyclo(Pro–Gly) cation mainly occur in the six-membered ring, while the five-membered ring remains almost unchanged, as can be seen from comparison with the neutral. The biggest change occurs in the C(1)—C(2) bond, which becomes longer in the radical cation.

Heat of formation of cyclo(Pro–Gly)

Two different homodesmotic reactions were designed for cyclo(Pro–Gly):

$$\text{cyclo(Pro–Gly)} + 4CH_3NH_2 + 6CH_3CH_3 \rightarrow 2CH_3CH_2NH_2 + 2CH_3CH_2CH_3 + 2CH_3CONH_2 + (CH_3)_2NH + (CH_3)_3N + (CH_3)_3CH \quad (1)$$

$$\text{cyclo(Pro–Gly)} + 3CH_3NH_2 + 3CH_3CH_3 \rightarrow CH_3CH_2NH_2 + CH_3CH_2CH_2NH_2 + CH_3CH(NH_2)CH_2CH_3 + CH_3CONHCH_3 + CH_3CON(CH_3)_2 \quad (2)$$

The calculated energy changes at 0 K for reactions (1) and (2) are listed in Table 1. We calculated total energies for relevant species in their ground states and

Table 1. Calculated energy changes (0 K, kcal mol^{-1} (1 kcal = 4.184 kJ)) for homodesmotic reactions of cyclo(Pro–Gly) and derived heat of formation of cyclo(Pro–Gly) at 0 K

Reaction	ΔE[a]	ΔH_f°[b]
Homodesmotic (1)	−3.9	−72.0
Homodesmotic (2)	−5.3	−71.9

[a] The energy changes of the reactions were calculated at the B3LYP/6–31G(d) level.
[b] The heat of formation was derived from available 0 K experimental values for other species participating in the reactions (see text).

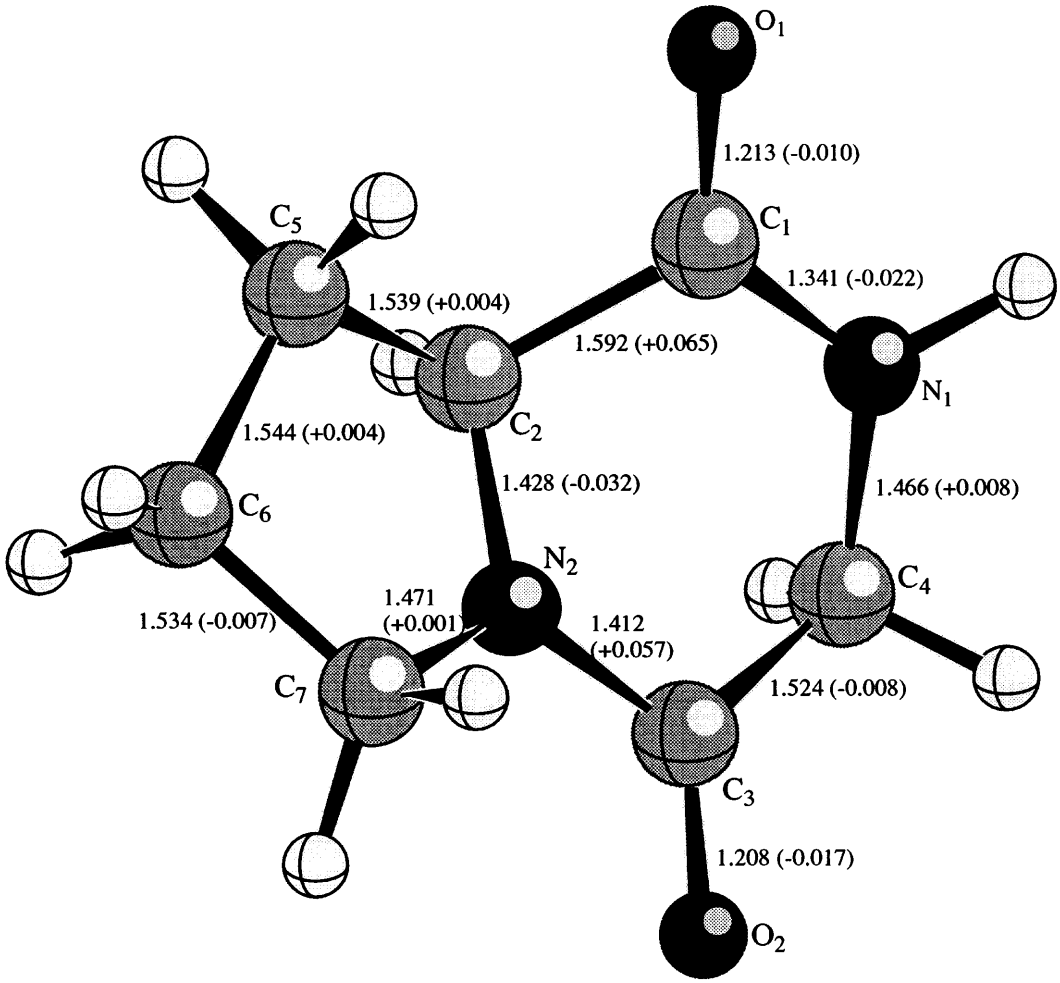

Figure 2. Geometry of cyclo(Pro–Gly) radical cation, optimized at the B3LYP/6–31G(d) level.

Table 2. Thermochemical data

Species	ΔH_f° (kcal mol^{-1}) 0 K	298 K	*IE* (eV)
Cyclo(Pro–Gly), $C_7H_{10}N_2O_2$	−72.0 ± 3.0	−81.4 ± 3.0	8.8 ± 0.1
Cyclo(Pro–Gly), $[C_7H_{10}N_2O_2]^{+\cdot}$	130.9 ± 3.0		
$[C_6H_9NO]^{+\cdot}$	⩽182.8 ± 5.0		

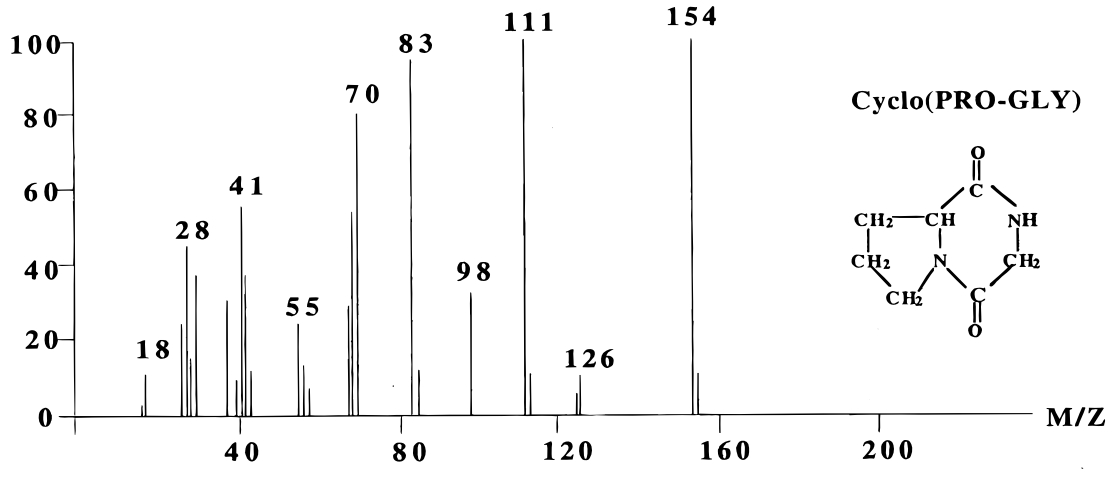

Figure 3. Mass spectrum of cyclo(Pro–Gly).

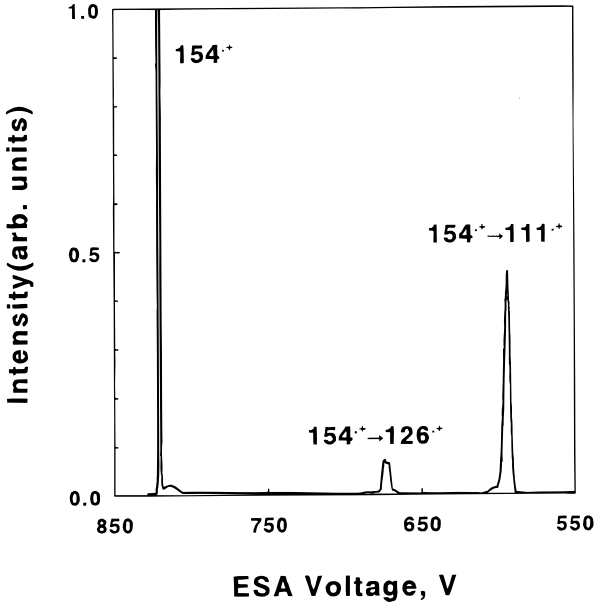

Figure 4. MIKE spectrum of the parent ion (m/z 154) of cyclo(Pro–Gly), obtained by scanning the electrostatic analyzer (ESA) voltage. The parent ion intensity is out of scale.

ZPVEs at the B3LYP/6–31G(d) level of theory. A scaling factor for the ZPVE, 0.9806, was adopted from Scott and Radom.[25] The heats of formation for all species at 0 K, which are needed to derive the heat of formation of cyclo(Pro–Gly), were converted from the 298.15 K value[29] with the scaled B3LYP/6–31G(d) vibrational frequencies. The heat of formation values of cyclo(Pro–Gly) at 0 K derived from reactions (1) and (2) are given in Table 1. The two values are almost equal at the B3LYP/6–31G(d) level. We therefore assign the heat of formation of cyclo(Pro–Gly) at 0 K the value -72.0 ± 3.0 kcal mol^{-1}. The heat of formation of cylco(Pro–Gly) at 298.15 K can be converted from the 0 K value with the scaled B3LYP/6–31G(d) vibrational frequencies by statistical mechanics methods, and the resultant values are given in Table 2.

Mass spectra and MIKE spectra

The mass spectrum of cyclo(Pro–Gly) is presented in Fig. 3. The two most intense peaks are at m/z 154 (the molecular ion) and m/z 111. The MIKE spectrum of the

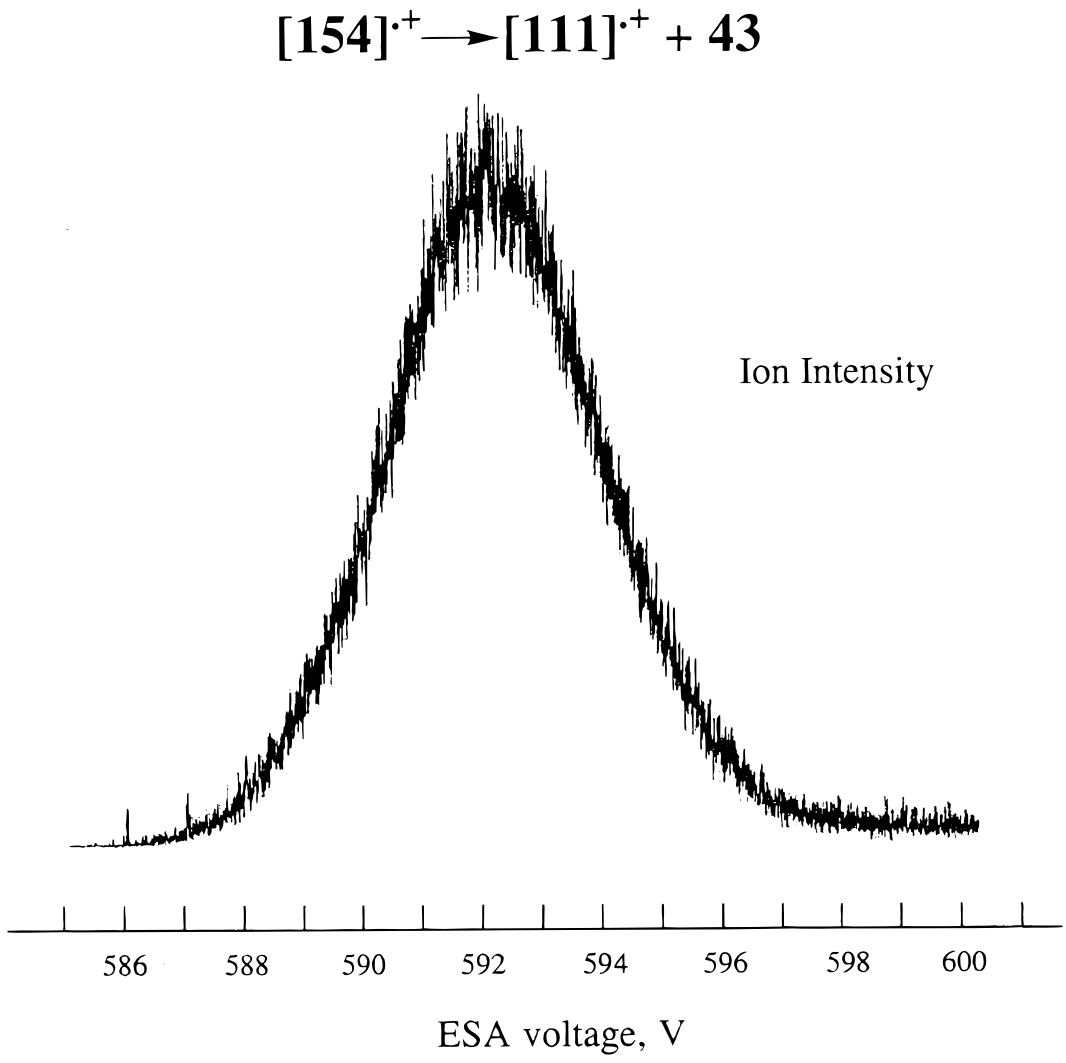

Figure 5. Metastable ion peak shape (second field-free region, ZAB-2F dissociation) for HNCO loss from cyclo(Pro–Gly). The parent ion beam passed at an energy of 7825 eV, corresponding to an ESA voltage of 821.64 V.

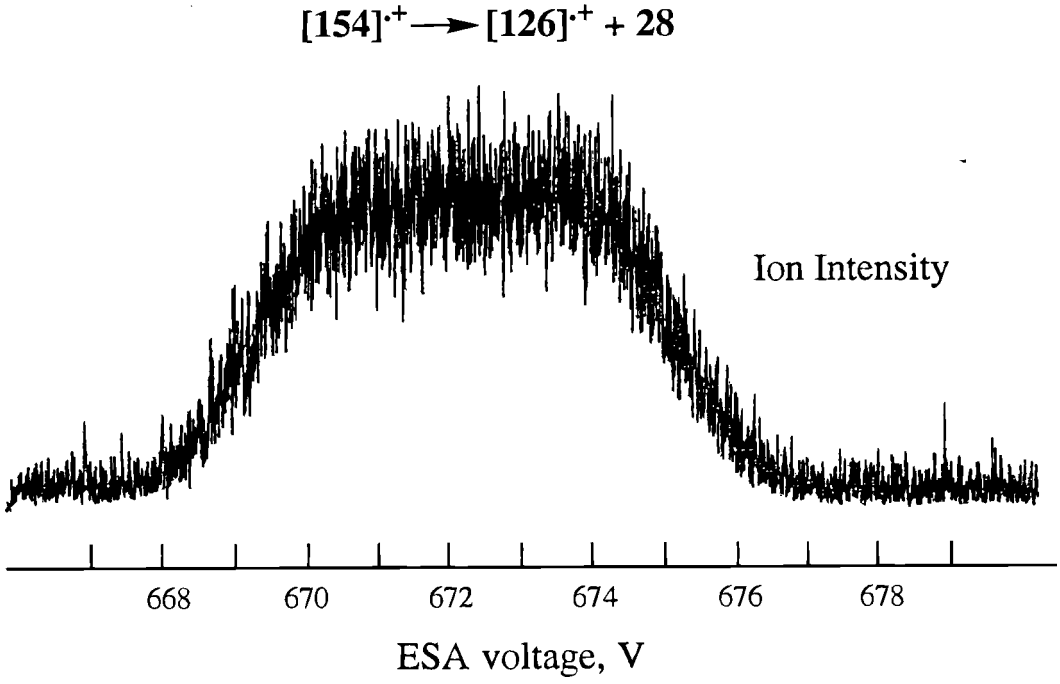

Figure 6. As Fig. 5, but for CO loss from cyclo(Pro–Gly).

cyclo(Pro–Gly) parent ion (*m/z* 154) demonstrates two peaks, at *m/z* 126 and 111, as shown in Fig. 4.

Several alternative reactions leading to $[M - 43]^{+\cdot}$ and $[M - 28]^{+\cdot}$ are possible. High-resolution mass measurements proved that *m/z* 111 is $[C_6H_9NO]^{+\cdot}$ and *m/z* 126 is $[C_6H_{10}N_2O]^{+\cdot}$ and the reactions are therefore

$$[C_7H_{10}N_2O_2]^{+\cdot} \rightarrow C_6H_9NO^{+\cdot} + HNCO \quad (3)$$

$$[C_7H_{10}N_2O_2]^{+\cdot} \rightarrow [C_6H_{10}N_2O]^{+\cdot} + CO \quad (4)$$

HNCO elimination was found to be at least five times more intense than CO elimination in the 70 eV mass spectrum (Fig. 3), both under MIKES (Fig. 4) and upon photoionization at 10.2 eV.

The metastable peak shapes for the reactions (3) and (4) are given in Fig. 5 and 6, respectively. The metastable peak shape for HNCO elimination (Fig. 5) is pseudo-Gaussian. This suggests that the source of the kinetic energy release (KER) is the excess non-fixed energy in the transition state and not a reverse activation energy barrier. The kinetic energy release distribution (KERD) obtained from the metastable peak shape is Boltzmann-like, as is seen in Fig. 7. The average KER deduced from the KERD is $T_{av} = 0.14$ eV. The flat-topped metastable peak shape for CO loss (Fig. 6) suggests a concerted elimination with a reverse activation

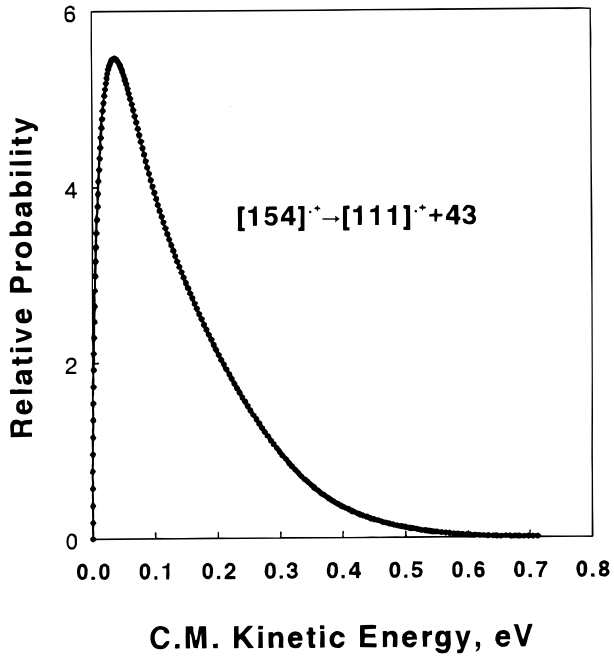

Figure 7. Product center of mass (CM) kinetic energy release distribution for metastable loss of HNCO from cyclo(Pro–Gly) radical cation.

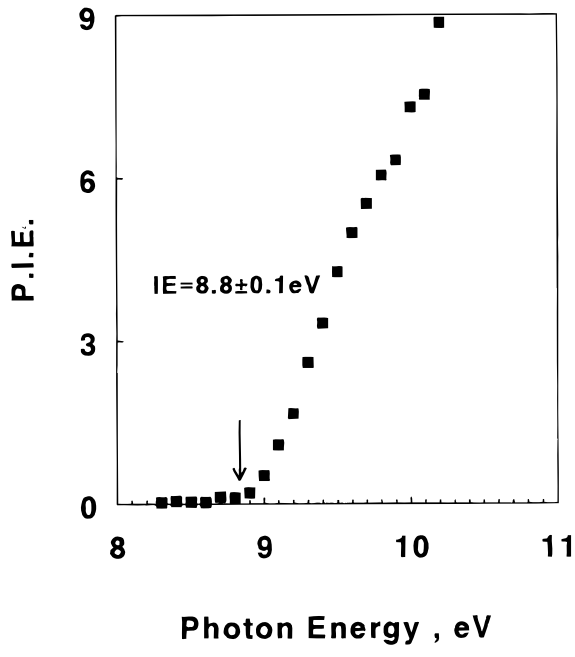

Figure 8. PIE curve for cyclo(Pro–Gly) parent ion (*m/z* 154).

energy. The width of the peak at half-height leads to a calculated KER of $T_{1/2} = 0.16$ eV.

Photoionization efficiency curves

PIE curves were measured on the vapor from the effusive Knudsen beam at 473 K. The PIE curve of the molecular ion of cyclo(Pro–Gly) demonstrates a sharp onset at 8.8 ± 0.1 eV, as shown in Fig. 8. The fragment ion (*m/z* 111) PIE curve is presented in Fig. 9. The appearance energy (9.9 ± 0.1 eV) is just 1.1 eV above the *IE*. A large kinetic shift is ruled out since the critical energy of activation, E_0, is not very high.

In the RRKM/QET modeling of the PIE curve, the C(1)—C(2) stretch was taken to be the reaction coordinate. Since the photoelectron spectrum (PES) of cyclo(Pro–Gly) is not available, we adopted the first derivative of the total PIE curve as the energy deposition function. The total PIE is the sum of the experimental parent and fragment PIEs. The thermal energy distribution is calculated from the scaled B3LYP/6–31G(d) neutral cyclo(Pro–Gly) vibrational frequencies and presented in Fig. 10. The average internal energy of cyclo(Pro–Gly) at 473 K is 0.46 eV. The calculated PIE curve is compared with the experimental curve in Fig. 9. Agreement between the experimental and computed PIE curves is seen to be very good. Figure 11 represents our calculated $k(E)$ dependence for the cyclo(Pro–Gly) ion dissociation. The reaction has a critical energy $E_0 = 1.2 \pm 0.1$ eV and an equivalent 1000 K entropy of activation $\Delta S‡ = 1.1 \pm 1.0$ eu.

Reaction mechanism and thermochemical information

The thermochemically calculated appearance energy for HNCO loss is 8.8 + 1.2 = 10.00 eV, as is shown in Fig. 9. The 'conventional' kinetic shift (CS) is defined[10,11] as the excess energy required to observe detectable (1%) dissociation within 10 μs, appropriate for conventional mass spectrometer appearance energy measurement. This can be calculated from the $k(E)$ dependence in Fig. 11. The predicted appearance energy is 10.24 eV for $k(E) = 10^3$ s^{-1}. The conventional kinetic shift (CS) is thus 0.24 eV. Because of the contribution of the thermal

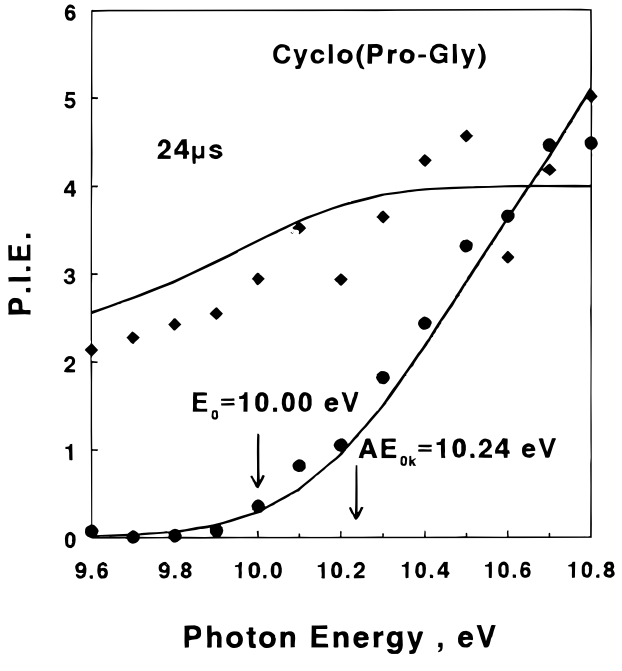

Figure 9. Experimental PIE curves ((●) fragment ion at *m/z* 111, (◆) parent ion at *m/z* 154) from cyclo(Pro–Gly) and calculated PIE curves (lines). The value $E_0 = 10.00$ eV corresponds to the sum of the ionization energy ($IE = 8.8$ eV) and the critical energy deduced from the modeling (1.2 eV). $AE_{0\,K} = 10.24$ eV is the calculated 0 K appearance energy which includes the kinetic shift.

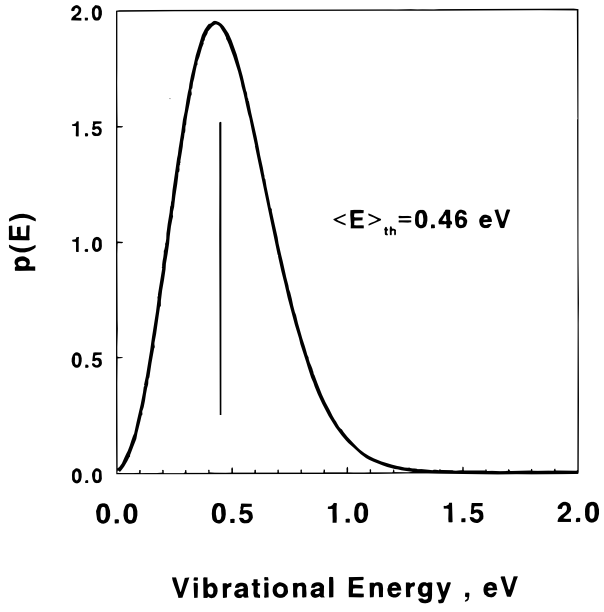

Figure 10. Thermal vibrational energy distribution of gaseous cyclo(Pro–Gly) at 473 K. The vertical line denotes the average vibrational internal energy. The calculation is based on the DFT vibrational frequencies.

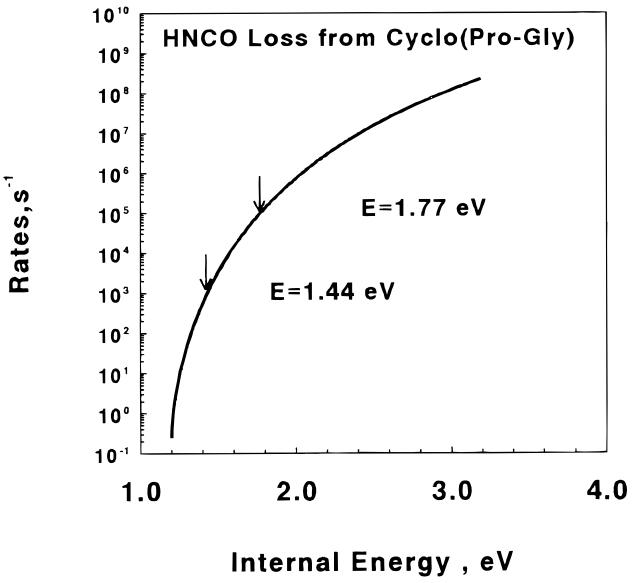

Figure 11. Calculated rate energy $k(E)$ dependence for cyclo(Pro–Gly) ion dissociation. The internal energies, 1.44 and 1.77 eV, shown are for $k(E)$ of 10^3 and 10^5 s^{-1}, respectively. $k(E) = 10^3$ s^{-1} corresponds to the observation of 1% fragmentation on a time-scale of microseconds and leads to an expected conventional kinetic shift of 10.24 − 10.00 eV = 0.24 eV. $k(E) = 10^5$ s^{-1} is the most probable rate constant in the field-free region of the mass spectrometer and leads to a calculated excess energy of 10.77 − 10.20 = 0.57 eV for metastable ions decomposing in flight.

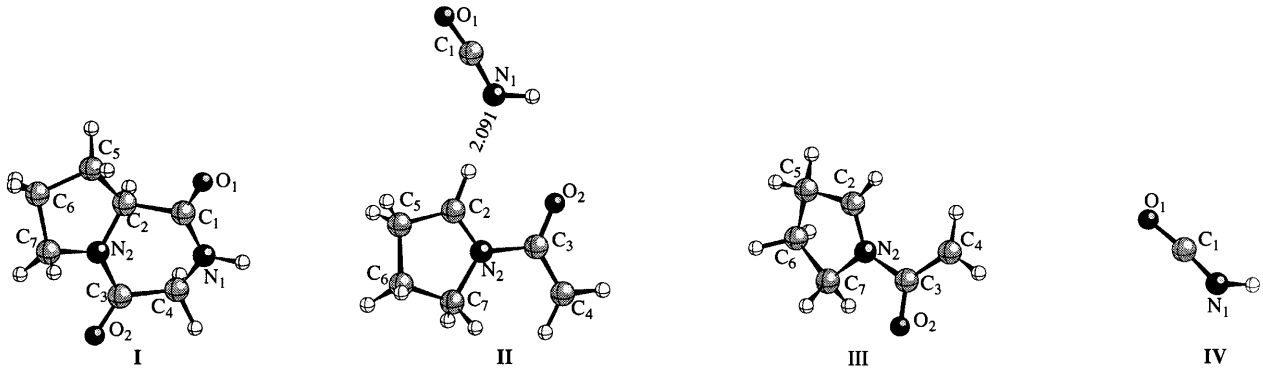

Figure 12. Optimized geometries of the $[C_6H_9NO]^{+\cdot}$–HNCO ion–dipole complex (**II**) and the products $[C_6H_9NO]^{+\cdot}$(**III**) and HNCO (**IV**) of reaction (3) calculated at the B3LYP/6–31G(d) level. The energies are **I** = −532.438 001, **II** = −532.417 515, **III** = −363.726 038 and **IV** = −168.677 509 hartree.

internal energy at 473 K, the experimental appearance energy is lower (see Fig. 9).

The excess energy in the metastable time window calculated from the $k(E)$ dependence in Fig. 11 is $1.77 - 1.20 = 0.57$ eV. However, the average kinetic energy release of 0.14 eV suggests a considerably larger excess energy, in view of the large number of degrees of freedom involved. The potential energy profile may possess two wells and the exit channel transition state of the two consecutive bond cleavages may lie below the transition state for the first cleavage which is rate determining. In this case, the appearance energy and critical energy deduced give only upper bounds of the reaction endothermicity.

The heat of formation of the cyclo(Pro–Gly) radical cation at 0 K can be calculated from the neutral value at 0 K and from the ionization energy to be 130.9 ± 3.0 kcal mol^{-1}. We can estimate an upper bound for the heat of formation of the product $[C_6H_9NO]^{+\cdot}$ ion from the parent ion $[C_7H_{10}N_2O_2]^{+\cdot}$ and HNCO[29] heats of formation and from our value for the critical energy of reaction (3). The value deduced and the other thermo-

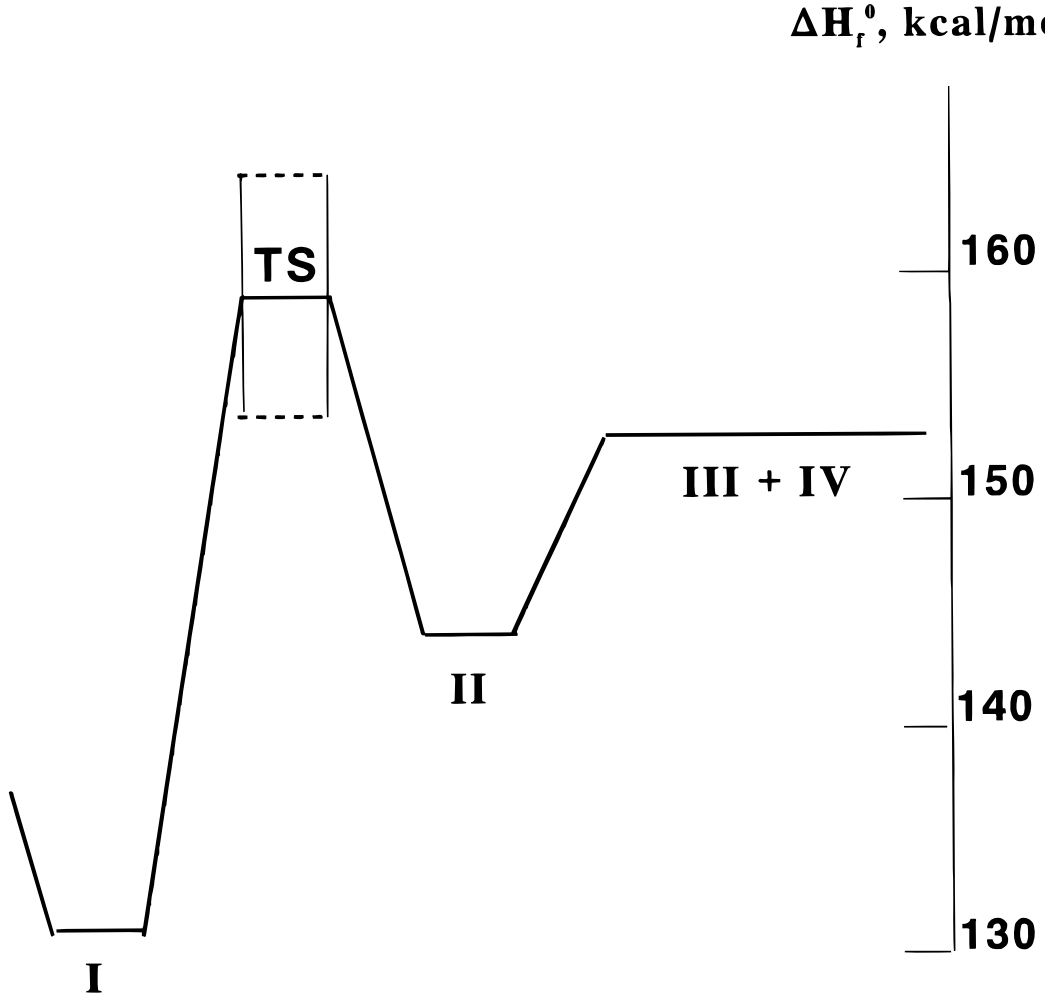

Figure 13. Potential energy profile for reaction (3) in $[cyclo(Pro–Gly)]^{+\cdot}$. The energy scale is the absolute heat of formation based on 0 K. The dashed lines give the accumulated error limits in the transition state (TS) heat of formation.

chemical data obtained in this work are summarized in Table 2.

The structure of the product ion $[C_6H_9NO]^{+\cdot}$ remains unknown. Theoretical calculations of $[C_9H_9NO]^{+\cdot}$ isomers and of the potential energy profile along the reaction coordinate of reaction (3) are desirable future developments.

Salient features of the potential energy profile

The salient features of the potential energy profile were calculated by DFT at the B3LYP/6–31G(d) level. Of particular interest to us was the possible role of an ion–dipole complex between the reaction products, in view of the high dipole moment of HNCO (calculated value = 2.2 D). Ion–dipole complexes have a particularly strong effect on the reaction dynamics in those cases in which they lie energetically below the reactant ion, e.g. in the case of H_2 loss from $[C_3H_7OH]^{+\cdot}$ [30] and $HO^{\cdot}$ loss from [*o*-nitrotoluene]$^{+\cdot}$.[31] We did not attempt a calculation of the transition state, but the energetics of the reactant ion **I**, the ion–dipole complex **II** and the products **III** and **IV** (see Fig. 12) combined with the experimental critical energy obtained from the RRKM modeling allowed us to construct a tentative profile (Fig. 13). The ion–dipole complex **II** lies at 12.86 kcal mol^{-1} higher energy than the [cyclo(Pro–Gly)]$^{+\cdot}$ reactant **I** and the transition state lies 0.26 eV higher than the calculated energy level of the products (27.7 *vs.* 21.6 kcal mol^{-1}); however, there are fairly large error limits on the heat of formation of the transition state (Fig. 13). The ion–dipole complex does not lie below the reactant ion and its density of states may therefore not have a strong influence on $k(E)$. However, it has been demonstrated[32] in the case of HCl elimination from [ethyl chloride]$^{+\cdot}$ that the ion–dipole complex which lies between the transition state and the products is ineffective in randomizing the excess energy among the product degrees of freedom. If this is the case for HNCO elimination from [cyclo(Pro–Gly)]$^{+\cdot}$, it can explain the relatively high kinetic energy release observed (0.14 eV), although the excess energy in the transition state is only $\sim 0.57 + 0.26$ eV ≈ 0.83 eV for the field-free region reaction of the VG-ZAB.

CONCLUSION

The major fragmentation channels of cyclo(Pro–Gly) cation at low energy were found to be HNCO and CO losses. The energetics of HNCO elimination were investigated by electron ionization MS/MS, PIMS and RRKM/QET modeling and DFT calculations. The heat of formation of cyclo(Pro–Gly) at 0 K was derived from homodesmotic reactions at the B3LYP/6–31G(d) level to be -72.0 ± 3.0 kcal mol^{-1}. The critical energy of HNCO loss from the cyclo(Pro–Gly) radical cation was determined to be 1.2 ± 0.1 eV.

Acknowledgements

We thank Drs D. Danovich, Jan M. L. Martin and U. Biedermann for helpful discussions and Dr F. Dubnikova for help with the DFT calculations. This research was supported by a grant from GIF, the German-Israeli Foundation for Scientific Research and Development.

REFERENCES

1. M. Henczi and D. F. Weaver, *Rapid Commun. Mass Spectrom.* **9**, 800 (1995).
2. J. P. Speir and I. J. Amster, *J. Am. Soc. Mass Spectrom.* **6**, 1069 (1995).
3. J. A. Carroll, J. Wu, T. Do and C. B. Lebrilla, in *Proceedings of the 42nd ASMS Conference on Mass Spectrometry and Allied Topics*, Chicago, IL, 1994, p. 475.
4. E. M. Marzluff, S. Campbell, M. T. Rodgers and J. L. Beauchamp, *J. Am. Chem. Soc.* **116**, 7787 (1994).
5. R. Weinkauf, P. Schanen, D. Yang, S. Soukara and E. W. Schlag, *J. Phys. Chem.* **99**, 11255 (1995).
6. L. L. Griffin and D. J. McAdoo, *J. Am. Soc. Mass Spectrom.* **4**, 11 (1993).
7. K. Eckart, *Mass Spectrom. Rev.* **13**, 23 (1994).
8. M. M. Cordero and C. Wesdemiotis, *Org. Mass Spectrom.* **29**, 382 (1994).
9. (a) R. G. Parr and W. Yang, *Density Functional Theory of Atoms and Molecules*. Oxford University Press, Oxford (1989); (b) N. C. Handy, in *Lecture Notes in Quantum Chemistry II*, edited by B. O. Roos, *Lecture Notes in Chemistry*, Vol. 64. Springer, Berlin (1994).
10. W. A. Chupka, *J. Chem. Phys.* **30**, 191 (1959).
11. (a) F. S. Huang and R. C. Dunbar, *J. Am. Chem. Soc.* **112**, 8167 (1990); (b) F. S. Huang and R. C. Dunbar, *Int. J. Mass Spectrom. Ion Processes* **109**, 151 (1991).
12. R. P. Morgan, J. H. Beynon, R. H. Bateman and B. M. Green, *Int. J. Mass Spectrom. Ion Processes* **28**, 171 (1978).
13. (a) J. L. Holmes and A. D. Osborne, *Int. J. Mass Spectrom. Ion Processes* **23**, 89 (1977); (b) C. Lifshitz and E. Tzidony, *Int. J. Mass Spectrom. Ion Processes* **39**, 181 (1981); (c) M. F. Jarrold, W. Wagner-Redeker, A. J. Illies, N. J. Kirchner and M. T. Bowers, *Int. J. Mass Spectrom. Ion Processes* **58**, 83 (1984).
14. C. Lifshitz, *Int. J. Mass Spectrom. Ion Processes* **106**, 159 (1991).
15. Y. Gotkis, M. Oleinikova, M. Naor and C. Lifshitz, *J. Phys. Chem.* **97**, 12282 (1993).
16. W. J. Hehre, L. Radom, P. V. R. Schleyer and J. A. Pople, *Ab initio Molecular Orbit Theory*. Wiley, New York (1986).
17. W. J. Hehre, R. Ditchfield, L. Radom and J. A. Pople, *J. Am. Chem. Soc.* **92**, 4796 (1970).
18. C. Heinemann, T. Muller, I. Apeloig and H. Schwarz, *J. Am. Chem. Soc.* **118**, 2023 (1996).
19. (a) P. George, M. Trachtman, C. W. Bock and A. M. Brett, *Tetrahedron* **32**, 317 (1976); (b) P. George, M. Trachtman, C. W. Bock and A. M. Brett, *J. Chem. Soc., Perkin Trans.* II, 1222 (1976); (c) P. George, C. W. Bock and M. Trachtman, in *Molecular Structure and Energetics*, edited by J. F. Liebman and A. Greenberg, Vol. 4. VCH, New York (1987).
20. M. N. Glukhovtsev, S. Laiter and A. J. Pross, *J. Phys. Chem.* **100**, 17801 (1996).
21. A. D. Becke, *J. Chem. Phys.* **98**, 5684 (1993).
22. C. Lee, W. Yang and R. G. Parr, *Phys. Rev. B* **37**, 185 (1988).
23. (a) J. M. L. Martin, J. El-Yazal and J. P. Francois, *Chem. Phys. Lett.* **242**, 570 (1995); (b) J. M. L. Martin, J. El-Yazal and J. P. Francois, *Mol. Phys.* **86**, 1437 (1995); (c) J. M. L. Martin, J. El-Yazal and J. P. Francois, *Chem. Phys. Lett.* **252**, 9 (1996); (d) J. M. L. Martin, J. El-Yazal and J. P. Francois, *Chem. Phys. Lett.* **255**, 7 (1996); (e) J. M. L. Martin, *Chem. Phys. Lett.* **262**, 97 (1996); (f) J. M. L. Martin, V. Aviyente and C. Lifshitz, *J. Phys. Chem.* **101**, 597 (1997).
24. G. Rauhut and P. Pulay, *J. Phys. Chem.* **99**, 3093 (1995).

25. A. P. Scott and L. Radom, *J. Phys. Chem.* **100**, 16502 (1996).
26. M. J. Frisch, G. W. Trucks, H. B. Schlegel, P. M. W. Gill, B. G. Johnson, M. A. Robb, J. R. Cheeseman, T. Keith, G. A. Petersson, J. A. Montgomery, K. Raghavachari, M. A. Al-Laham, V. G. Zakrzewski, J. V. Ortiz, J. B. Foresman, J. Cioslowski, B. B. Stefanov, A. Nanayakkara, M. Challacombe, C. Y. Peng, P. Y. Ayala, W. Chen, M. W. Wong, J. L. Andres, E. S. Replogle, R. Gomperts, R. L. Martin, D. J. Fox, J. S. Binkley, D. J. DeFrees, J. Baker, J. P. Stewart, M. Head-Gordon, C. Gonzalez and J. A. Pople, *Gaussian 94, Revision B.1*. Gaussian, Pittsburgh, PA (1995).
27. I. Gotkis and C. Lifshitz, *Org. Mass Spectrom.* **28**, 372 (1993).
28. W. L. Hase and D. L. Bunker, *A General RRKM Program, QCPE No. 234*. Chemistry Department, Indiana University, Bloomington, IN.
29. S. G. Lias, J. E. Bartmess, J. F. Liebman, J. L. Holmes, R. D. Levin and W. G. Mallard, *J. Phys. Chem. Ref. Data* **17**, Suppl. 1 (1988).
30. J. D. Shao, T. Baer, J. C. Morrow and M. Fraser-Monteiro, *J. Chem. Phys.* **87**, 5242 (1987).
31. J. D. Shao and T. Baer, *Int. J. Mass Spectrom. Ion Processes* **86**, 357 (1988).
32. J. A. Booze, K.-M. Weitzel and T. Baer, *J. Chem. Phys.* **94**, 3649 (1991).

